Phase Behavior and Morphology in Blends of Poly(L-lactic acid) and Poly(butylene succinate)

Jun Wuk Park, Seung Soon Im

Department of Fiber & Polymer Engineering, College of Engineering, Hanyang University, 17 Haengdang-dong, Seongdong-gu, Seoul, 133-791, South Korea

ABSTRACT: Blends of poly(L-lactic acid) (PLA) and poly-(butylene succinate) (PBS) were prepared with various compositions by a melt-mixing method and the phase behavior, miscibility, and morphology were investigated using differential scanning calorimetry, wide-angle X-ray diffraction, small-angle X-ray scattering techniques, and polarized optical microscopy. The blend system exhibited a single glass transition over the entire composition range and its temperature decreased with an increasing weight fraction of the PBS component, but this depression was not significantly large. The DSC thermograms showed two distinct melting peaks over the entire composition range, indicating that these materials was classified as semicrystalline/semicrystalline blends. A depression of the equilibrium melting point of the PLA component was observed and the interaction parameter between PLA and PBS showed a negative value of −0.15, which was derived using the Flory–Huggins equation. Small-angle X-ray scattering revealed that, in the blend system, the PBS component was expelled out of the interlamellar regions of PLA, which led to a significant decrease of a long-period, amorphous layer thickness of PLA. For more than a 40% PBS content, significant crystallization-induced phase separation was observed by polarized optical microscopy. © 2002 Wiley Periodicals, Inc. J Appl Polym Sci 86: 647–655, 2002

Key words: poly(L-lactic acid); poly(butylene succinate); blends; miscibility; morphology

INTRODUCTION

Both poly(L-lactic acid) (PLA) and poly(butylene succinate) (PBS) are known as biodegradable polyesters with good mechanical properties and degradability. Especially, PLA has been widely used in biomaterial applications because of its good biocompatability and various physical properties. But its brittleness is a major defect for many applications. Moreover, the relatively high price of the intermediate lactide lowers the possibility of their commercialization. Therefore, to modify various properties or to lower the price, studies on PLA blends with other polymers were carried out. PLA was reported to be miscible with other stereoisomers such as poly(DL-lactic acid), and the blends had varying properties according to the mixing ratio.[1,2] It is also known that PLA is able to form miscible blends with various polymers such as poly-(ethylene oxide),[3] poly(vinyl acetate),[4] and poly(ethylene glycol).[5]

The miscibility, crystallization behavior, and morphology of the PLA/PBS blend have not been reported in the literature. These polymers are both crystallizable and have a relatively rapid crystallization rate. So, we expect that this blend system is a semicrystalline/semicrystalline system, which can exhibit a complicated phase behavior including semicrystalline/amorphous and semicrystalline/semicrystalline states. At a temperature between the melting points of the two semicrystalline polymers, the morphology of this blend is actually a semicrystalline/amorphous system and the amorphous component can reside between the interlamellar[6] and interfibrillar[7] regions or can even be rejected from the spherulites.[8] The semicrystalline/semicrystalline states have much more complex morphologies. After primary crystallization of one component in the semicrystalline/semicrystalline blend system, secondary lamellar can be formed at different locations in the spherulites. There are two models: the dual lamellar stack model[9] formed between stacks of lamellae separated from the primary formed lamellar stacks and the lamellar insertion model[10,11] formed between the primary lamellae within the same stack. Recently, semicrystalline/semicrystalline polymer blends of poly(vinylidene fluoride)/poly(1,4-butylene adipate)[12–15] and polycaprolactone/polycarbonate[16–18] were reported in the literature, including the miscibility, the overall phase behavior, the crystallization behavior, and the morphology, in considerable detail.

In this study, PLA was blended with PBS and its miscibility, phase behavior, crystallization behavior,

---

and morphology were investigated using differential scanning calorimetry (DSC), small-angle X-ray scattering (SAXS), wide-angle X-ray diffraction (WAXD), and polarized optical microscopy. In particular, this study was focused on the phase behavior and morphology in the semicrystalline/semicrystalline phase to gain a better understanding of its complex mixtures.

EXPERIMENTAL

Materials and sample preparation

The PLA samples used in this research were supplied by the Korea Institute of Science and Technology, with weight-average molecular weights of approximately 367,000, and were purified by reprecipitation using chloroform as the solvent and methanol as the precipitant. The PBS ($M_w = 1.2 \times 10^5$) sample was obtained from the SAEHAN Industries (Korea) and used as received. PLA and PBS were dried under a vacuum at 40°C for 3 days.

Blends of PLA and PBS were prepared by melt-mixing using a twin-screw Haake Reomix 600 at 60 rpm and 190°C for 5 min. The mixing compositions were 100/0, 90/10, 80/20, 70/30, 60/40, 50/50, 30/70, and 100/0 wt % of PLA/PBS. After blending, all the samples were cooled to room temperature under an air atmosphere.

Films with a thickness of 0.2 mm were prepared using a hot press at 185°C, a hold pressure of 3000 psi, and a hold time of 3 min. For a quenched sample, prepared films were quenched in cold water (~0°C) and then dried under a vacuum at room temperature for 3 days to remove water thoroughly and stored in a desiccater with P_2O_5. But for the crystallized sample, prepared films were put in the oven at the desired temperature and isothermal-crystallized for 12 h.

DSC

Thermal characteristics of the blends were measured using a Perkin–Elmer DSC-7. Sealed aluminum sample pans containing 5–10 mg of the blend materials were used in all the experiments. At the beginning of each experiment, except for crystallized samples, the samples were heated at 190°C for 5 min to eliminate their thermal history and then rapidly cooled to 0°C. The actual measurement was performed during a second heating from 0 to 200°C at a heating rate of 10°C/min.

WAXD and SAXS measurements

WAXD measurements were performed using an X-ray diffractometer (Rigaku Denki D-Max2000, Japan) operated at 40 W and 160 mA and a scan speed of 5°/min with a 2θ range of 5°–40°. The X-ray source was a
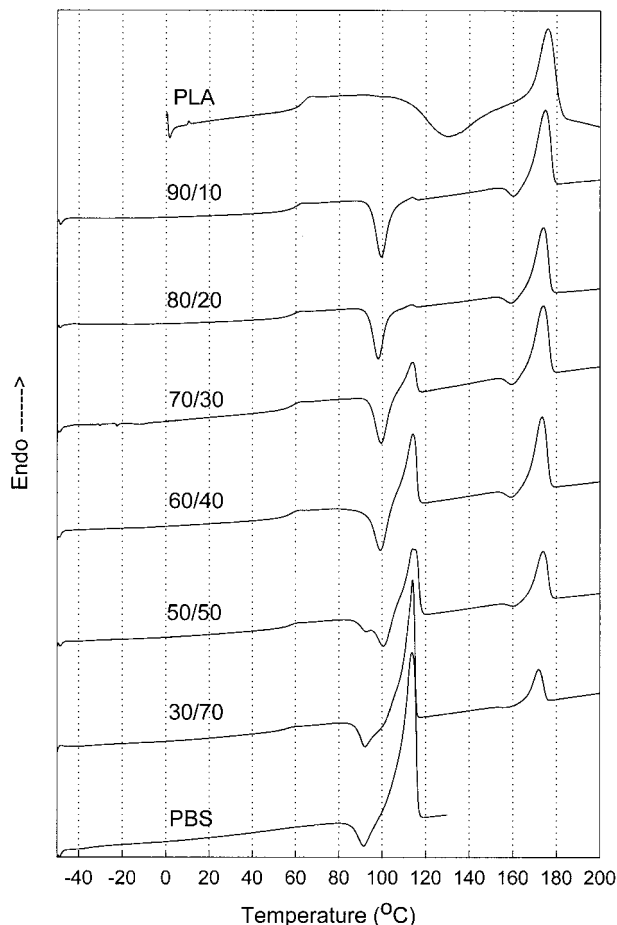

Figure 1 DSC thermograms of PLA/PBS blends.

18-kW rotating anode X-ray generator equipped with a rotating anode Cu target. SAXS measurements were carried out using the same apparatus at the same power with a 2θ range of 0.1°–5°.

Polarized optical microscopy

The sample was first melted on a hot stage at 190°C for 5 min and then rapidly transferred to another hot stage equilibrated at a given crystallization temperature. After annealing for given time periods, the spherulite morphology was observed using a Nikon polarized light microscope (OPTIPOTO-POL).

RESULTS AND DISCUSSION

DSC

Figure 1 shows DSC thermograms of PLA/PBS blends and their characteristic values are denoted in Table I. The DSC thermogram of pure PLA shows a broad crystallization peak between 110 and 150°C and a melting peak at about 176°C. However, for pure PBS, a sharp exothermal peak and melting peak are observed at 92 and 114°C, respectively, which are lower

TABLE I
Thermal Characteristics of PLA/PBS Blends

Mixing ratios of PLA/PBS (w/w)	PBS		PLA			
	T_g	T_m	T_g	T_m	ΔH_f (J/g)	χ (%)
100/0	—	—	64.2	176.1	27.1	28.5
90/10	—	113.6	60.2	174.7	39.6	41.6
80/20	—	113.4	60.0	173.9	36.1	38.0
70/30	—	113.9	59.3	173.8	35.1	36.9
60/40	—	114.1	58.4	173.4	34.8	36.6
50/50	—	114.0	58.4	173.9	35.1	36.9
30/70	—	114.0	56.6	171.9	34.3	36.1
0/100	−34.0	113.7	—	—	—	—

than those for PLA. Particularly, their T_g's show a great difference of approximately 100°. But the blend system exhibits a single glass transition over the entire composition range and its temperature decreases with an increasing weight fraction of the PBS component. This may be taken as evidence of miscibility in the amorphous phase. But this depression with an increasing PBS composition is not so large as to fit into the classical Fox equation or the Gordon–Taylor equation.[19] It is well known that PBS undergoes crystallization at room temperature. So, the DSC heating or cooling rate is slow enough for PBS to undergo crystallization, and due to the presence of crystallinities, the composition of the amorphous phase is different from the overall blend composition, that is, the composition of PBS is smaller than that of PLA in the amorphous phase. Therefore, the miscibility of two polymers could not be determined with only changes of the glass transition temperature.

The thermograms show two distinct melting peaks over the entire composition range, indicating that these materials are classified as semicrystalline/semicrystalline blends. In spite of a significant difference in the exothermal peak temperatures between PLA and PBS, for a PBS composition of only 10 wt %, the exothermal peak shows a sharp single peak at 100°C. In addition, the bulk crystallinity (χ %) greatly increased in comparison with that of pure PLA. These results show that PBS was a good plasticizer for PLA. It has been reported, for other polymers, that plasticizers contribute to an improvement in the crystallinity of a polymer.[20] Naturally functionalized oils have been found to improve the crystallization behavior of poly(ethlene terephthalate).[21] In the case of PLA, it was reported that the addition of citrate esters as plasticizers led to an increase in crystallinity and also that enhanced molecular mobility due to the presence of a plasticizer could cause an increase in crystallinity.[22]

When the PBS composition is more than 50 wt %, the exothermal peaks exhibit single peaks with a shoulder. For PBS-rich blends, it is possible that, owing to a faster crystallization rate and a lower crystal-

lization temperature of the PBS component than those of the PLA component, the PBS component first undergoes crystallization at a lower temperature before the crystallization of PLA.

The correct T_m (PBS), T_c, and ΔH could not be obtained because of their overlapping around 90–110°C. But the T_m of the PLA component can be precisely obtained and it decreased with an increase in the PBS composition. Generally, in miscible blends, the melting point of the crystalline component is lowered in comparison with the pure polymer as a result of a favorably thermodynamic interaction. Flory–Huggins theory[23] is known as a method for estimating polymer miscibility by the depression of the melting point. Thus, to determine the miscibility of PLA and PBS, this method was applied to the PLA/PBS blend systems. The equilibrium melting point of a polymer was most conveniently determined using Hoffman–Weeks analysis.[24] This method involves isothermal crystallization of the sample at various temperatures and plotting the observed melting point as a function of T_c. To apply Flory–Huggins theory to the PLA/PBS blend system, isothermal crystallization was carried out at the temperature range of 120–160°C. In this temperature range, only the PLA component undergoes crystallization, leading to a two-phase morphology of a mixed amorphous phase and a crystalline phase.

Figure 2 shows Hoffman–Weeks plots for PLA in its blends with PBS at various compositions. The equilibrium melting point T_m^0 is obtained from the intersection of this line with the $T_m = T_c$ equation. T_m^0 for pure PLA was about 203°C, which is slightly lower than previously reported values in the range from 207 to 212°C.[25] In the blends, the equilibrium melting point of the PLA phase decreases largely in the early stage, but this depression is decreased with increasing PBS content. The maximum extent of this melting-point depression is 15° in the 30/70 blend, where the T_m^0 is 188°C.

According to the Flory–Huggins theory, the melting-point depression of the crystallizable component in the compatible blend with a noncrystallizable component can be written as follows:

$$\frac{1}{T_m^0 \text{ (blend)}} - \frac{1}{T_m^0 \text{ (pure)}} = -\frac{RV_2}{\Delta H^0 V_1}$$

$$\times \left[\frac{\ln\phi_2}{m_2} + \left(\frac{1}{m_2} - \frac{1}{m_1}\right)\phi_1 + \chi_{12}\phi_1^2 \right] \quad (1)$$

where ΔH^0 is the heat of fusion of the crystalline component; V, the molar volume of the repeat unit; and m and ϕ, the degree of polymerization and the volume fraction, respectively. To determine the interaction parameter χ_{12}, eq. (1) can be rewritten as follows:

$$-\left[\frac{\Delta H^0 V_1}{RV_2} \left(\frac{1}{T_m^0 \text{ (blend)}} - \frac{1}{T_m^0 \text{ (pure)}}\right) \frac{\ln\phi_2}{m_2} \right.$$

$$\left. + \left(\frac{1}{m_2} - \frac{1}{m_1}\right)\phi_1 \right] = \chi_{12}\phi_1^2 \quad (2)$$

Subscripts 1 and 2 refer to the noncrystalline (PBS) and crystalline (PLA) polymers, respectively. If the interaction parameter is independent of the blend composition, a plot of the left-hand side versus ϕ_1^2 in eq. (2) should give a straight line, the slope of which is equal to degree χ_{12}. The values of the left-hand side of eq. (2) from the experimental melting-point temperature was calculated using the following parameter values: $\Delta H^0 = 120 \text{ J/cm}^3$ (ref. 26), $m_1 = 698$, $m_2 = 5097$, $V_1 = 152.2$ cm^3/mol, and $V_2 = 57.14$ cm^3/mol. The volume fractions were calculated from the weight fraction using the densities of PLA and PBS.

Figure 3 shows plots of eq. (2) using the experimental melting temperature of the PLA component in the PLA/PBS blends. A straight line has some deviation with the actual values and the intercept at $\phi_1^2 = 0$ is not a negligible value. This implies that the interaction
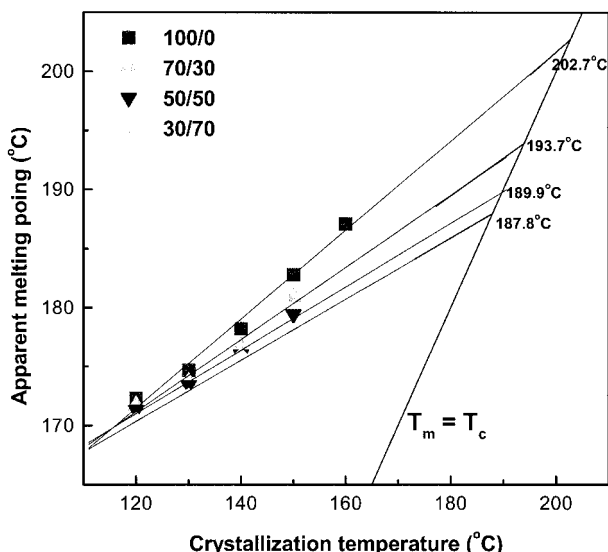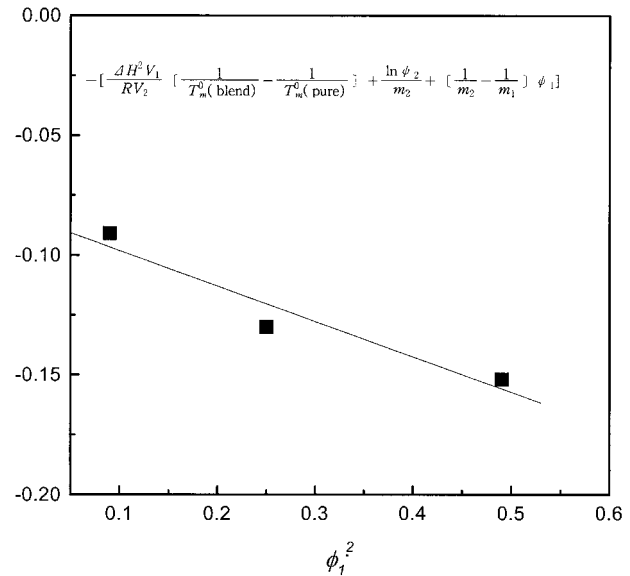
Figure 3 Plots according to Flory—Huggins equation for PLA/PBS blends at various compositions.

parameter is not independent of the blend composition or that the depression of the melting point is influenced not only by the interaction between two polymers but also by the morphological effects, such as a smaller lamellar thickness. But its slope is a certainly negative value of -0.15. This indicates that the PLA/PBS polymer blends are thermodynamically miscible and that PLA and PBS can form a compatible mixture in the melt state above the melting point of the PLA component.

WAXD

The samples with various compositions were isothermally crystallized at 100°C for 12 h and their WAXD patterns are presented in Figure 4. Pure PLA shows a typical pattern with a strong diffraction peak of 16.5° and a weak peak of 19°, corresponding with the (110) and (203) planes, respectively. The pattern for pure PBS shows a strong peak of (110) at 22.9° and weak peaks of (021), (020), and (111) at 22.0°, 19.7°, and 29.3°, respectively. For the blends, new peaks or shifts of peaks as a result of cocrystallization between the two components or modification in the unit cell parameters of PLA and PBS do not appear. This indicates that cocrystallization is not expected to occur between the two polymers and each crystallization of the two components occurs separately, leading to a phase separation from the mixture to form a pure phase, that is, a crystallization-induced phase separation.

Figure 2 Hoffman–Weeks plots for PLA in its blends with PBS at various compositions.

SAXS

Smoothed and Lorentz-corrected scattering profiles for the PLA/PBS blends at various compositions are
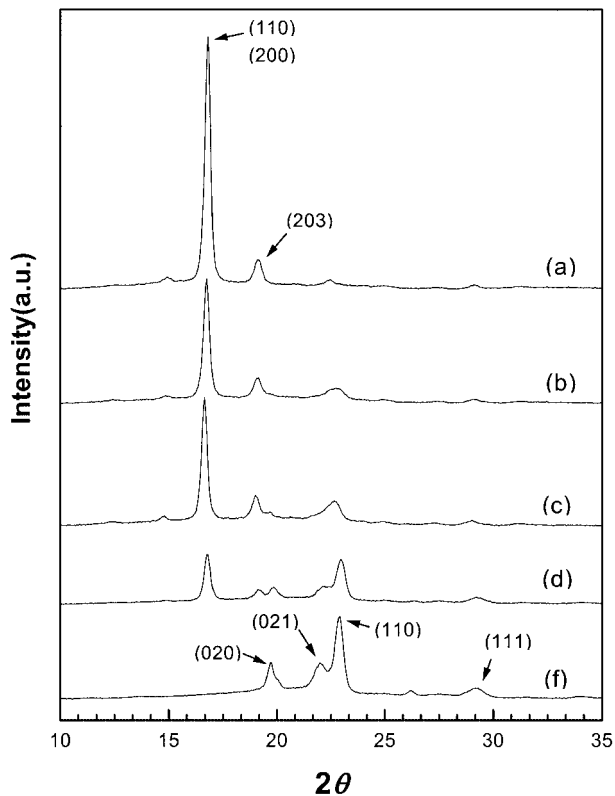
Figure 4 WAXD patterns of PLA/PBS blends isothermally crystallized at 100°C for 12 h: (a) 100/0; (b) 70/30; (c) 50/50; (d) 30/70; (f) 0/100.
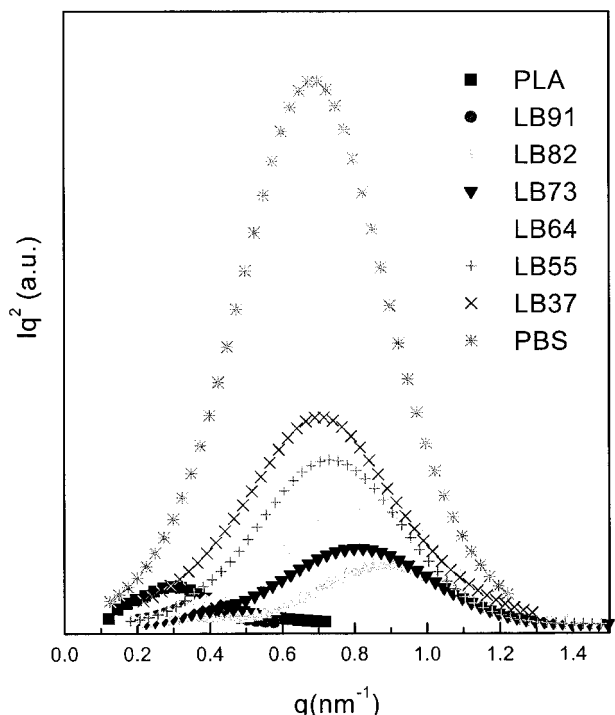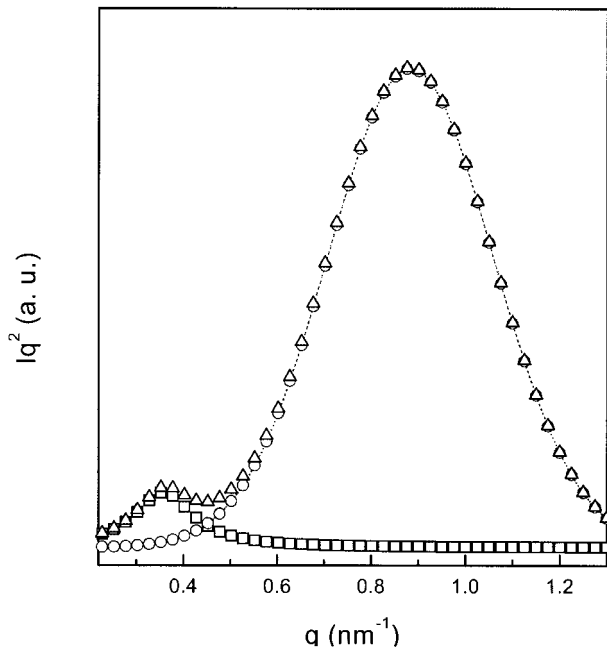

Figure 6 Peak separation of smoothed and Lorentz-corrected SAXS profile of PLA/PBS 80/20 blends, isothermally crystallized at 100°C for 12 h.

shown in Figure 5. Pure PLA exhibits a weak scattering peak around $q = 0.1$–0.5 nm^{-1}, while pure PBS exhibits a very strong scattering peak at a higher scattering angle, indicating that the electron density difference between the crystalline and amorphous regions in PBS is much larger than that in PLA, but in the case of a long period, PLA has higher value than that of PBS. For the PLA/PBS blend systems, a clear scattering shoulder is observed at PBS compositions
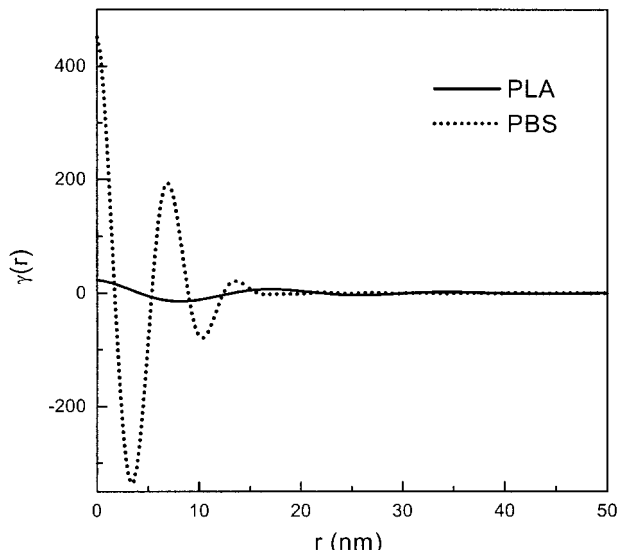

Figure 5 Smoothed and Lorentz-corrected SAXS profiles of PLA, PBS, and PLA/PBS blends, isothermally crystallized at 100°C for 12 h.

Figure 7 Typical one-dimensional correlation function for 80/20 PLA/PBS blends, isothermally crystallized at 100°C for 12 h.
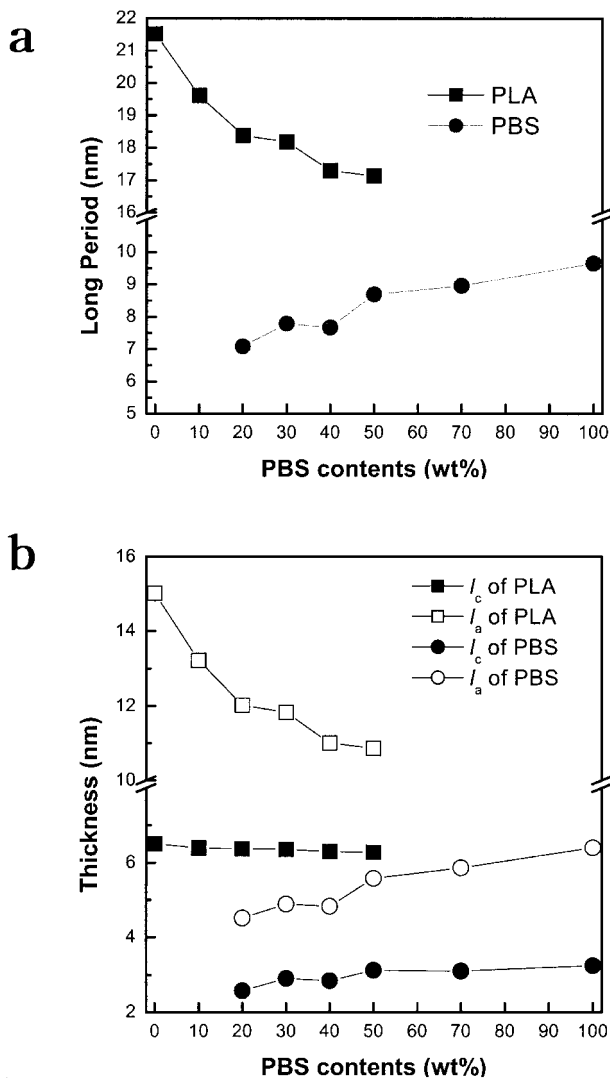
Figure 8 Plot of (a) long period (*L*) and (b) lamellar thickness (*l_c*) and amorphous layer thickness (*l_a*) as a function of PBS content for PLA/PBS blends, isothermally crystallized at 100°C for 12 h.

from 20 to 50 wt %. In particular, it appears as a well-defined peak, almost a double peak, for the 80/20 blend. From these results, we think that the blend system has a dual lamellar stack in this composition range. After primary crystallization of one component in a semicrystalline/semicrystalline blend system, a secondary lamellar can be formed at different locations in the spherulites, as shown schematically in Figure 6. According to the dual lamellar stack model,[9] secondary crystallization leads to the formation of stacks of lamellae separated from the primary formed lamellar stacks. In the lamellar insertion,[10,11] thin secondary lamellae are formed between the primary lamellae within the same stack. If thin lamellar are formed within the same stack as the primary lamellae, this would result in a broad single scattering peak at a higher scattering angle in the SAXS patterns. Thus, the

lamellar insertion model is not valid in the PLA/PBS blend system with double or single shoulder scattering peaks and one can assume that the secondary lamellae are located at stacks separated from the primary formed lamellar stacks according to the dual lamellar stack model.

With this assumption, peaks of the SAXS patterns in Figure 5 were separated into PLA and PBS components using a peak-separation computer program. Figure 6 shows the peak separation of the SAXS pattern for 80/20 blend. It is found that scattering peaks from PLA and PBS lamellar stacks are well separated. With each separated peak, the average lamellar thickness and amorphous-phase thickness were calculated from the normalized one-dimensional correlation function [$\gamma(r)$], evaluated from the scattered intensity $I(q)$ by the following equation[27]:

$$\gamma(r) = \left(\frac{1}{2\pi}\right)^2 \int q^2 I(q)\cos(qr)dq \qquad (3)$$

where $q = 4\ \pi/\lambda\ \sin(\theta/2)$ (θ is the scattering angle) and r is the correlation distance. As the experimentally accessible q range is finite, it was necessary to extend the data to both lower and higher q values. The intensity versus q data were linearly extrapolated from the smallest measured q value to zero. Large q values were damped to infinite q by using the Porod law (q^{-4} decay).[28]

Figure 7 exhibits a typical correlation function of the PLA and PBS components for a 80/20 blend. The average long period L was determined by the Bragg relation $L = 2\pi/q_{max}$ in Lorrenz-corrected SAXS patterns, and the average lamellar thickness (l_c) was determined from x-axis values of an intersection point between the tangent line at $\gamma(r) = 0$ and the tangent
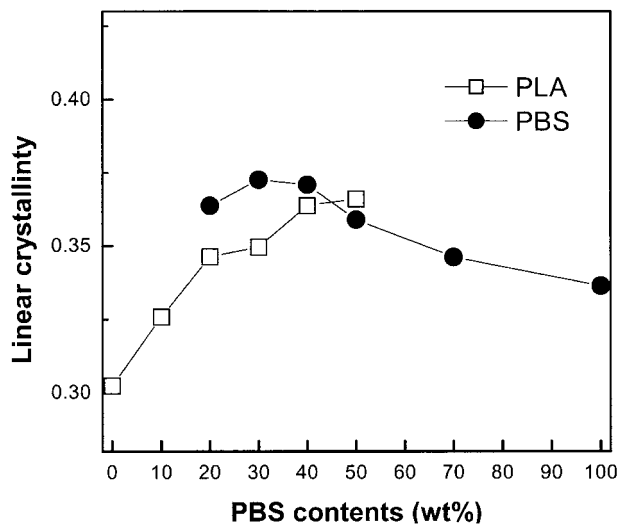

Figure 9 Effect of linear crystallinities on PBS content for PLA/PBS blends, isothermally crystallized at 100°C for 12 h.
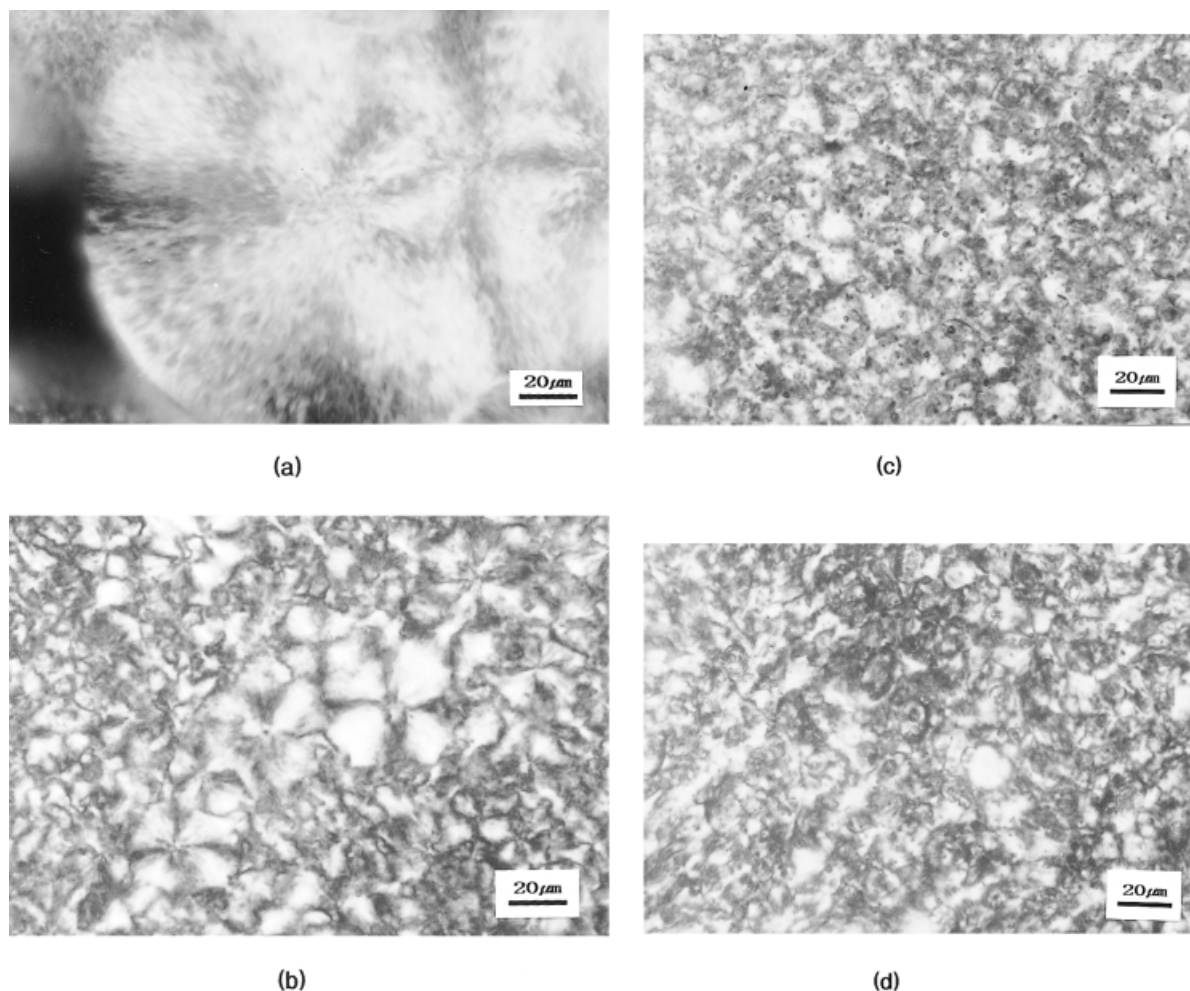
Figure 10 Polarized optical micrographs of PLA/PBS blends, isothermally crystallized at 100°C for 12 h: (a) 100/0; (b) 90/10; (c) 80/20; (d) 70/30 (e) 60/40; (f) 50/50; (g) 30/70 (h) 0/100. [Color figure can be viewed in the online issue, which is available at www.interscience. wiley.com.]

line at the first minimum in the correlation curve and the amorphous phase thickness l_a $(= L = l_c)$ could be calculated with L and l_c.

The long period (L), the average lamellar thickness (l_c), and the amorphous phase thickness l_a at all composition ranges in PLA/PBS blends are shown in Figure 8. The long period of PLA decreases with an increasing PBS content and that of PBS also decreases with an increasing PLA content. In particular, the depression of the long period for PLA is larger than that for PBS. This is due to a large decrease of the amorphous phase thickness compared to that of the lamellar thickness, which slightly decreases. In general, during crystallization in the melt-miscible crystalline/amorphous blend, there are two forces: the entropic force associated with the tendency to resume random-coiled conformation and the crystallization driving force of crystallizable segments in the interlamellar regions.[6,29] These two forces compete against the favorable interaction between the amorphous component and the amorphous portion of the crystal-

line polymer in the interlamellar regions. Exclusion of the amorphous component out of the interlamellar regions is, consequently, governed by the magnitude of the interaction, the interlamellar distance, and the degree of supercooling. Kinetically, chain diffusivity may also be an important factor. If the diffusion rate of the amorphous component is relatively slower than is the crystal growth rate, diluent molecules may be trapped inside the interlamellar regions before they had a chance to diffuse out. In this case, the long period and amorphous layer thickness are expected not to decrease. On the contrary, if the diffusion rate of impurity is relatively faster than is the crystal growth rate, impurities may leach out of the interlamellar zones, leading to a decrease of the long period and the amorphous layer thickness. Accordingly, we suggest that the large decrease of the long period and the amorphous layer thickness of PLA components in the PLA/PBS blends is due to a faster diffusion rate of the PBS component than the crystal growth rate of the PLA components.
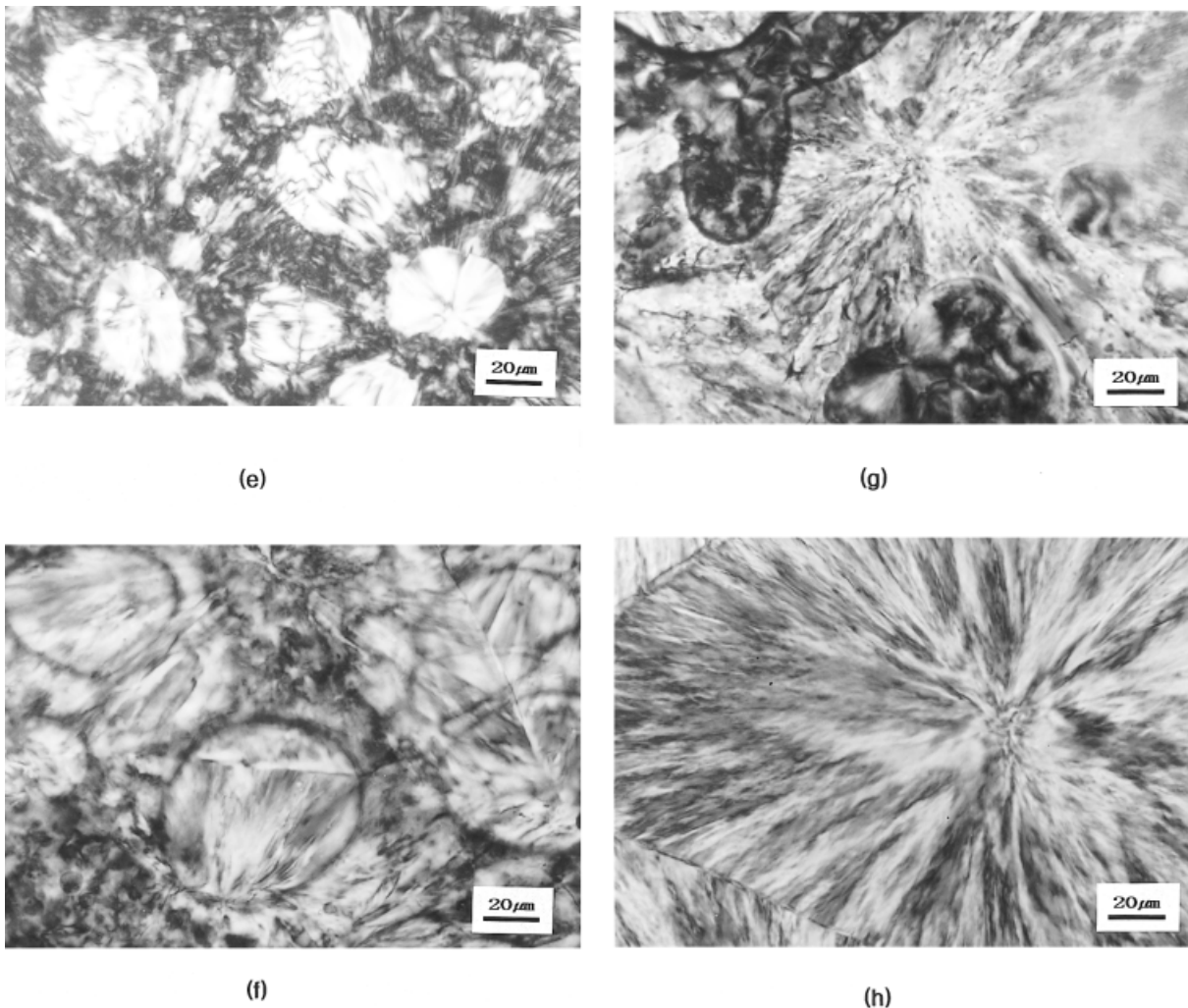
Figure 10   (*Continued from the previous page*)

Spherulitic morphologies

For PBS, all the long period, lamellar thickness, and amorphous layer thickness decrease with an increasing PLA content. In particular, a decrease of the amorphous layer thickness is smaller than that of PLA. Because the crystal growth rate of PBS is very fast and the diffusion rate of PLA with a higher molecular weight is lower than that of PBS, we think that the PLA component cannot thoroughly be expelled out of the PBS interlamellar region, leading to a relatively slight decrease of the amorphous layer thickness of PBS.

Figure 9 shows the linear crystallinities ($= l_c/L$) calculated from the long period and the lamellar thickness. The linear crystallinities of PLA increase with an increasing PBS content and those of PBS also increase with an increasing PLA content. The increment for PLA is larger than that for PBS, as a result of the larger decrement of the amorphous layer thickness for PLA than that for PBS. In conclusion, this increment of the linear crystallinities indicates that most of the amorphous mixtures of the two component locate in interfibrillar or interspherulitic regions.

Figure 10 shows polarized optical micrographs of PLA/PBS blends at various blend compositions, after complete crystallization at 100°C for 12 h. The spherulites of pure PLA show a good fibril structure grown radially and the average radius of the spherulites is about 140 μm. For pure PBS, well-grown spherulites, which are very tightly spaced, are observed and the average radius is larger than that of PLA. For the PLA/PBS blend with less than a PBS composition of 30 wt %, a large number of small spherulites are observed and their sizes and shapes were much smaller and less regular than those of pure PLA. In this composition range, because the PBS crystals, which are expected to crystallize first, cannot grow, largely as a result of the low content, significant crystallization-induced phase separation did not take place. But over the PBS compositon of 40 wt %, large spherulites of PBS and small sphelulites of PLA are shown. In particular, for 30/70 blend, huge spheru-

lites of PBS are observed in a continuous phase and PLA crystal domains are isolated.

CONCLUSIONS

1. The blend system exhibited a single glass transition over the entire composition range and its temperature decreased with an increasing weight fraction of the PBS component, but this depression was not significantly large. The DSC thermograms showed two distinct melting peaks over the entire composition range, indicating that these materials were classified as semicrystalline/semicrystalline blends.
2. A depression of the equilibrium melting point of the PLA component was observed and the interaction parameter between PLA and PBS showed a negative value of −0.15, which was derived using the Flory–Huggins equation.
3. Small-angle X-ray scattering revealed that, in the blend system, the PBS component was expelled out of the interlamellar regions of PLA, which led to a significant decrease of the long-period, amorphous layer thickness of PLA.
4. From polarized optical microscopic measurements, significant crystallization-induced phase separation was observed for more than a 40% PBS content.

References

1. Tsuji, H.; Ikada, Y. Polymer 1996, 37, 595.
2. Perego, G.; Domenico, F; Bastioli, C. J Appl Polym Sci 1996, 59, 37.
3. Nijienhuis, A. J.; Colstee, E.; Grijpma, D. W.; Pennings, A. J. Polymer 1996, 37, 5849.
4. Gajria, A. M.; Dave, V.; Gross, R. A.; McCarthy, S. P. Polymer 1996, 37, 437.
5. Sheth, M.; Kumar, R. A.; Dave, V.; Gross, R. A.; McCarthy, S. P. J Appl Polym Sci 1997, 66, 1495.
6. Russell, T. P.; Ito, H.; Wignall, G. D. Macromolecules 1988, 21, 1703.
7. Warner, F. P.; Stein R. S.; MacKnight, W. J. J Polym Sci Polym Phys Ed 1977, 15, 2113.
8. Keith, H. D.; Padden, F. J. J Appl Phys 1964, 35, 1270.
9. Verma, R.; Marand H.; Hsiao, B. Macromolecules 1996, 29, 7767.
10. Kruger, K. N.; Zachmann, H. G. Macromolecules 1993, 26, 5202.
11. Hsiao, B.; Gardner, K. C.; Wu, D.; Chu, B. Polymer 1993, 34, 3986.
12. Penning, J. P.; Manley, R. St. J. Macromolecules 1996, 29, 77.
13. Penning, J. P.; Manley, R. St. J. Macromolecules 1996, 29, 84.
14. Fujita, K.; Kyu, T.; Manley, R. St. J. Macromolecules 1996, 29, 91.
15. Liu, L. Z.; Chu, B.; Penning, J. P.; Manley, R. St. J. Macromolecules 1997, 30, 4398.
16. Cheung, Y. W.; Stein, R. S. Macromolecules 1994, 27, 2512.
17. Cheung, Y. W.; Stein, R. S.; Lin, J. S.; Wignall, G. D. Macromolecules 1994, 27, 2520.
18. Cheung, Y. W.; Stein, R. S.; Chu, B.; Wu, G. Macromolecules 1994, 27, 3589.
19. Gordon, M.; Taylor, J. S. J Appl Chem 1952, 2, 493.
20. Gachter, R.; Muller, H. Plastics Additives Handbook, 3rd ed.; Hanser: New York, 1990; Chapter 5.
21. Barrett, L. W.; Sperling, L. H. Proc ACS Div PMSE 1991, 65, 345.
22. Labrecque, L. V.; Kumar, R. A.; Dave, V.; Gross, R. A.; Mccarthy, S. P. J Appl Polym Sci 1997, 66, 1507.
23. Nishi, T.; Wang, T. T. Macromolecules 1975, 8, 909.
24. Hoffman, J. D.; Weeks, J. J. J Res Natl Bur Stand A 1962, 66, 13.
25. Tsuji, H.; Ikada, Y. Polymer 1995, 36, 2709.
26. Hoffman, J. D.; Miller, R. L.; Marand, H.; Roitman, D. B. Macromolecules 1992, 25, 2221.
27. Strobl, G. R.; Schneider, M. J.; Voight-Martin, I. G. J Polym Sci Polym Phys Ed 1980, 18, 1361.
28. Balta-Calleja, F. J.; Vonk, C. G. X-ray Scattering of Synthetic Polymers; Elsevier: New York, 1989; Chapter 7.3.
29. Chen, H. L.; Li, L. J.; Lin, T. L. Macromolecules 1998, 31, 2255.